December 2014

Sediment Profile Imaging Report

Demonstration of *in-situ* Treatment of Contaminated Sediments with Reactive Amendments: Post-Cap Survey #3




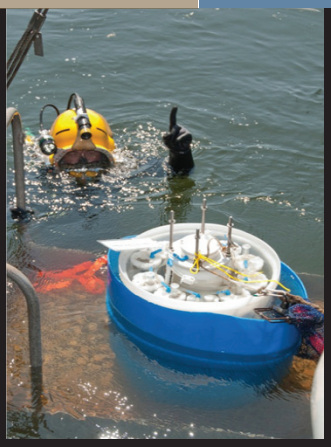


Prepared for

Hart Crowser, Inc.
1700 Westlake Avenue North
Suite 200
Seattle, WA 98109-3856

Hart Crowser Job Number 1789702,
Work Order #2

Prepared by

Germano & Associates, Inc.
12100 SE 46th Place
Bellevue, WA 98006

Sediment Profile Imaging Report

DEMONSTRATION OF *IN-SITU* TREATMENT OF CONTAMINATED SEDIMENTS WITH REACTIVE AMENDMENTS: POST CAP SURVEY #3

Prepared for

Hart Crowser, Inc.
1700 Westlake Avenue North, Suite 200
Seattle, WA 98109-3856

Hart Crowser Job Number 1789702, Work Order #2

Prepared by

Germano & Associates, Inc.
12100 SE 46th Place
Bellevue, WA 98006

December, 2014

TABLE OF CONTENTS

LIST OF FIGURES

1.0
INTRODUCTION

As part of a multidisciplinary effort to investigate the feasibility of treating contaminated sediments in active Department of Defense (DoD) harbors, Germano & Associates, Inc. (G&A) performed a Sediment Profile Imaging (SPI) survey around Pier 7 at the Puget Sound Naval Shipyard & Intermediate Maintenance Facility (PSNS & IMF) Bremerton site. The purpose of this SPI survey was to continue to monitor recolonization and benthic habitat conditions at a total of 50 stations following placement of a reactive amendment cap placed on the sediment surface. This was the third post-cap monitoring survey performed as part of this multidisciplinary demonstration research project.

2.0
MATERIALS AND METHODS

Between October 14-16, 2012, 141 tons of AquaGate +PAC™ were placed in the target area for remediation under and around Pier 7 at PSNS & IMF Bremerton site (Johnston et al. 2013). The AquaGate +PAC™ consisted of an aggregate (limestone pebble) core surrounded with a mixture of powdered activated carbon (PAC) held together by a clay (bentonite) binder that was designed to release from aggregate once placed on the sea floor (Johnston et al. 2013). A pre-placement baseline SPI survey was conducted Aug 16-17, 2012 (G&A 2013a) and post-placement SPI surveys were conducted 2 weeks (Oct 30-31, 2012; G&A 2013b), 10 months (Aug 13-14, 2013; G&A 2014), and 22 months (July 29-30, 2014; this report) after placement. For each of these surveys, scientists from G&A collected a series of sediment profile images at a total of 42 stations and mapped the presence and thickness of the cap layer. During the 10 month and 22 month monitoring surveys, scientists from G&A collected sediment profile images from the same 42 stations as the baseline and initial post-cap surveys in August 2012 October 2012, respectively, as well as an additional 8 stations (Figure 1). The primary objective of the post-cap surveys was to monitor the recolonization of the cap as well as the active reworking of the reactive amendment into the sediment by resident infauna. For all surveys, two different versions of an Ocean Imaging Systems Model 3731 sediment profile camera were used; a standard SPI system using a surrounding frame that was deployed from a vessel (Figure 2), and a hand-held aluminum SPI system (Figure 3) deployed by PSNS & IMF divers for stations that were located under the pier and inaccessible for sampling with a vessel.

SPI was developed almost four decades ago as a rapid reconnaissance tool for characterizing physical, chemical, and biological seafloor processes and has been used in numerous seafloor surveys throughout North America, Asia, Europe, and Africa (Rhoads and Germano 1982, 1986, 1990; Revelas et al. 1987; Diaz and Schaffner, 1988; Valente et al. 1992; Germano et al. 2011). The sediment profile camera works like an inverted periscope. A Nikon D7000 16.2-megapixel Single Lens Reflex (SLR) camera with two 8-gigabyte secure digital (SD) cards is mounted horizontally inside a watertight housing on top of a wedge-shaped prism. The prism has a Plexiglas® faceplate at the front with a mirror placed at a 45° angle at the back. The camera lens looks down at the mirror, which is reflecting the image from the faceplate. The prism has an internal strobe mounted inside at the back of the wedge to provide illumination for the image; this chamber is filled with distilled water, so the camera always has an optically clear path. This wedge assembly is mounted on a moveable carriage within a stainless steel frame. The frame is lowered to the seafloor on a winch wire, and the tension on the wire keeps the prism in its "up" position. When the frame comes to rest on the seafloor, the winch wire goes slack (see Figure 2) and the camera prism descends into the sediment at a slow, controlled rate by the dampening action of a hydraulic piston so as not to disturb the sediment-water

interface. On the way down, it trips a trigger that activates a time-delay circuit of variable length (operator-selected) to allow the camera to penetrate the seafloor before any image is taken. The knife-sharp edge of the prism transects the sediment, and the prism penetrates the bottom. The strobe is discharged after an appropriate time delay to obtain a cross-sectional image of the upper 20 cm of the sediment column. The resulting images give the viewer the same perspective as looking through the side of an aquarium half-filled with sediment. After the first image is obtained at the first location, the camera is then raised up about 2 to 3 meters off the bottom to allow the strobe to recharge; a wiper blade mounted on the frame removes any mud adhering to the faceplate. The strobe recharges within 5 seconds, and the camera is ready to be lowered again for a replicate image. Surveys can be accomplished rapidly by "pogo-sticking" the camera across an area of seafloor while recording positional fixes on the surface vessel.

The hand-held SPI system (Figure 3) works on the same design, except that there is no time delay once the watertight switch is activated by the diver after the prism is inserted into the sediment. There is no wiper blade on the hand-held system, so the diver needs to clean the faceplate of the camera prism manually with a scrub brush after each image is taken.

Two types of adjustments to the SPI system are typically made in the field: physical adjustments to the chassis stop collars on the frame-deployed system or adding/subtracting lead weights to the chassis to control penetration in harder or softer sediments, and electronic software adjustments to the Nikon D7000 to control camera settings. Camera settings (f-stop, shutter speed, ISO equivalents, digital file format, color balance, etc.) are selectable through a water-tight USB port on the camera housing and Nikon Control Pro® software. At the beginning of the survey, the time on both of the sediment profile cameras' internal data loggers was synchronized with the clock on the sampling vessel to local time. Details of the camera settings for each digital image are available in the associated parameters file embedded in the electronic image file; for this survey, the ISO-equivalent was set at 800. The additional camera settings used were as follows: shutter speed was 1/250, f8, white balance set to flash, color mode to Adobe RGB, sharpening to none, noise reduction off, and storage in compressed raw Nikon Electronic Format (NEF) files (approximately 20 MB each). Electronic files were converted to high-resolution jpeg (14-bit) format files (49278 x 3264 pixels) using Nikon Capture NX2® software (Version 2.3.7.).

Typically, three replicate images were taken at each station at the vessel-deployed frame stations, while 2 replicate images were taken by the divers at each of the under-pier stations; each SPI replicate is identified by the time recorded on the digital image file in the camera and in the field log on the vessel. The SD card was immediately surrendered at the completion of the survey to PSNS & IMF for review and approval for public distribution. The unique time stamp on the digital image was then cross-checked with the time stamp recorded in the written sample logs. After the images were cleared for public

release, they were re-named with the appropriate station name based on the time stamp on each image.

Test exposures of the Kodak® Color Separation Guide (Publication No. Q-13) were made on deck at the beginning of the survey to verify that all internal electronic systems were working to design specifications and to provide a color standard against which final images could be checked for proper color balance. A spare camera and charged battery were carried in the field at all times to insure uninterrupted sample acquisition. After deployment of the camera at each station, the frame counter was checked to make sure that the requisite number of replicates had been taken. In addition, a prism penetration depth indicator on the camera frame was checked to verify that the optical prism had actually penetrated the bottom to a sufficient depth. If images were missed (frame counter indicator or verification from digital download) or the penetration depth was insufficient (penetration indicator), chassis stops were adjusted and/or weights were added or removed, and additional replicate images were taken. Changes in prism weight amounts, the presence or absence of mud doors, and chassis stop positions were recorded for each replicate image.

Following completion of the field operations, the raw NEF image files were converted to high-resolution Joint Photographic Experts Group (jpeg) format files using the minimal amount of image file compression. Once converted to jpeg format, the intensity histogram (RGB channel) for each image was adjusted in Adobe Photoshop® to maximize contrast without distortion. The jpeg images were then imported to Sigmascan Pro® (Aspire Software International) for image calibration and analysis. Calibration information was determined by measuring 1-cm gradations from the Kodak® Color Separation Guide. This calibration information was applied to all SPI images analyzed. Linear and area measurements were recorded as number of pixels and converted to scientific units using the calibration information.

Measured parameters were recorded on a Microsoft® Excel© spreadsheet. G&A's senior scientist (Dr. J. Germano) subsequently checked all these data as an independent quality assurance/quality control review of the measurements before final interpretation was performed.

2.1 MEASURING, INTERPRETING, AND MAPPING SPI PARAMETERS

2.1.1 Prism Penetration Depth

The SPI prism penetration depth was measured from the bottom of the image to the sediment-water interface. The area of the entire cross-sectional sedimentary portion of the image was digitized, and this number was divided by the calibrated linear width of the image to determine the average penetration depth.

Prism penetration is a noteworthy parameter; if the number of weights used in the camera is held constant throughout a survey, the camera functions as a static-load penetrometer. Comparative penetration values from sites of similar grain size give an indication of the relative water content of the sediment. Highly bioturbated sediments and rapidly accumulating sediments tend to have the highest water contents and greatest prism penetration depths.

The depth of penetration also reflects the bearing capacity and shear strength of the sediments. Overconsolidated or relic sediments and shell-bearing sands resist camera penetration. Highly bioturbated, sulfitic, or methanogenic muds are the least consolidated, and deep penetration is typical. Seasonal changes in camera prism penetration have been observed at the same station in other studies and are related to the control of sediment geotechnical properties by bioturbation (Rhoads and Boyer 1982). The effect of water temperature on bioturbation rates appears to be important in controlling both biogenic surface relief and prism penetration depth (Rhoads and Germano 1982).

2.1.2 Thickness of Depositional Layers

Because of the camera's unique design, SPI can be used to detect the thickness of dredged material and depositional layers (like the reactive amendment). SPI is effective in measuring layers ranging in thickness from 1 mm to 20 cm (the height of the SPI optical window). During image analysis, the thickness of the newly deposited sedimentary layers can be determined by measuring the distance between the pre- and post-placement sediment-water interface. Recently deposited material is usually evident because of its unique optical reflectance and/or color relative to the underlying material representing the pre-operational surface. Also, in most cases, the point of contact between the two layers is clearly visible as a textural change in sediment composition, facilitating measurement of the thickness of the newly deposited layer. In this study, the presence of the aggregate core and/or activated (black) carbon were used to indicate the presence of the reactive amendment.

2.1.3 Apparent Redox Potential Discontinuity Depth

Aerobic near-surface marine sediments typically have higher reflectance relative to underlying hypoxic or anoxic sediments. Surface sands washed free of mud also have higher optical reflectance than underlying muddy sands. These differences in optical reflectance are readily apparent in SPI images; the oxidized surface sediment contains particles coated with ferric hydroxide (an olive or tan color when associated with particles), while reduced and muddy sediments below this oxygenated layer are darker, generally gray to black (Fenchel 1969; Lyle 1983). The boundary between the colored ferric hydroxide surface sediment and underlying gray to black sediment is called the apparent redox potential discontinuity (aRPD).

The depth of the aRPD in the sediment column is an important time-integrator of dissolved oxygen conditions within sediment porewaters. In the absence of bioturbating organisms, this high reflectance layer (in muds) will typically reach a thickness of 2 mm below the sediment-water interface (Rhoads 1974). This depth is related to the supply rate of molecular oxygen by diffusion into the bottom and the consumption of that oxygen by the sediment and associated microflora. In sediments that have very high sediment oxygen demand (SOD), the sediment may lack a high reflectance layer even when the overlying water column is aerobic.

In the presence of bioturbating macrofauna, the thickness of the high reflectance layer may be several centimeters. The relationship between the thickness of this high reflectance layer and the presence or absence of free molecular oxygen in the associated porewaters must be considered with caution. The actual RPD is the boundary or horizon that separates the positive reduction potential (Eh) region of the sediment column from the underlying negative Eh region. The exact location of this Eh = 0 boundary can be determined accurately only with microelectrodes; hence, the relationship between the change in optical reflectance, as imaged with the SPI camera, and the actual RPD can be determined only by making the appropriate *in situ* Eh measurements. For this reason, the optical reflectance boundary, as imaged, was described in this study as the "apparent" RPD and it was mapped as a mean value. In general, the depth of the actual Eh = 0 horizon will be either equal to or slightly shallower than the depth of the optical reflectance boundary (Rosenberg et al., 2001). This is because bioturbating organisms can mix ferric hydroxide-coated particles downward into the bottom below the Eh = 0 horizon. As a result, the mean aRPD depth can be used as an estimate of the depth of porewater exchange, usually through porewater irrigation (bioturbation). Biogenic particle mixing depths can be estimated by measuring the maximum and minimum depths of imaged feeding voids in the sediment column. This parameter represents the particle mixing depths of head-down feeders, mainly polychaetes.

The rate of depression of the aRPD within the sediment is relatively slow in organic-rich muds, on the order of 200 to 300 micrometers per day; therefore this parameter has a long time constant (Germano and Rhoads 1984). The rebound in the aRPD is also slow (Germano 1983). Measurable changes in the aRPD depth using the SPI optical technique can be detected over periods of 1 or 2 months. This parameter is used effectively to document changes (or gradients) that develop over a seasonal or yearly cycle related to water temperature effects on bioturbation rates, seasonal hypoxia, SOD, and infaunal recruitment. Time-series RPD measurements following a disturbance can be a critical diagnostic element in monitoring the degree of recolonization in an area by the ambient benthos (Rhoads and Germano 1986).

The mean aRPD depth also can be affected by local erosion. The peaks of disposal mounds commonly are scoured by divergent flow over the mound. This scouring can wash away fines and shell or gravel lag deposits, and can result in very thin surface

oxidized layer. During storm periods, erosion may completely remove any evidence of the aRPD (Fredette et al. 1988).

Another important characteristic of the aRPD is the contrast in reflectance at this boundary. This contrast is related to the interactions among the degree of organic loading, the bioturbation activity in the sediment, and the concentrations of bottom-water dissolved oxygen in an area. High inputs of labile organic material increase SOD and, subsequently, sulfate reduction rates and the associated abundance of sulfide end products. This results in more highly reduced, lower-reflectance sediments at depth and higher aRPD contrasts. In a region of generally low aRPD contrasts, images with high aRPD contrasts indicate localized sites of relatively large inputs of organic-rich material such as phytoplankton, other naturally-occurring organic detritus, dredged material, or sewage sludge.

Because the determination of the aRPD requires discrimination of optical contrast between oxidized and reduced particles, it is difficult, if not impossible, to determine the depth of the aRPD in well-sorted sands of any size that have little to no silt or organic matter in them (Painter et al, 2007). When using SPI technology on sand bottoms, little information other than grain-size, prism penetration depth, and boundary roughness values can be measured; while oxygen has no doubt penetrated the sand beneath the sediment-water interface just due to physical forcing factors acting on surface roughness elements (Ziebis et al., 1996; Huettel et al., 1998), estimates of the mean aRPD depths in these types of sediments are indeterminate with conventional white light photography.

2.1.4 Infaunal Successional Stage

The mapping of infaunal successional stages is readily accomplished with SPI technology. These stages are recognized in SPI images by the presence of dense assemblages of near-surface polychaetes and/or the presence of subsurface feeding voids; both may be present in the same image. Mapping of successional stages is based on the theory that organism-sediment interactions in fine-grained sediments follow a predictable sequence after a major seafloor perturbation. This theory states that primary succession results in "the predictable appearance of macrobenthic invertebrates belonging to specific functional types following a benthic disturbance. These invertebrates interact with sediment in specific ways. Because functional types are the biological units of interest..., our definition does not demand a sequential appearance of particular invertebrate species or genera" (Rhoads and Boyer 1982). This theory is presented in Pearson and Rosenberg (1978) and further developed in Rhoads and Germano (1982) and Rhoads and Boyer (1982).

This continuum of change in animal communities after a disturbance (primary succession) has been divided subjectively into four stages: Stage 0, indicative of a sediment column that is largely devoid of macrofauna, occurs immediately following a physical disturbance or in close proximity to an organic enrichment source; Stage 1 is the

initial community of tiny, densely populated polychaete assemblages; Stage 2 is the start of the transition to head-down deposit feeders; and Stage 3 is the mature, equilibrium community of deep-dwelling, head-down deposit feeders (Figure 4).

After an area of bottom is disturbed by natural or anthropogenic events, the first invertebrate assemblage (Stage 1) appears within days after the disturbance. Stage 1 consists of assemblages of tiny tube-dwelling marine polychaetes that reach population densities of 10^4 to 10^6 individuals per m^2. These animals feed at or near the sediment-water interface and physically stabilize or bind the sediment surface by producing a mucous "glue" that they use to build their tubes. Sometimes deposited dredged material layers contain Stage 1 tubes still attached to mud clasts from their location of origin; these transported individuals are considered as part of the *in situ* fauna in our assignment of successional stages.

If there are no repeated disturbances to the newly colonized area, then these initial tube-dwelling suspension or surface-deposit feeding taxa are followed by burrowing, head-down deposit-feeders that rework the sediment deeper and deeper over time and mix oxygen from the overlying water into the sediment. The animals in these later-appearing communities (Stage 2 or 3) are larger, have lower overall population densities (10 to 100 individuals per m^2), and can rework the sediments to depths of 3 to 20 cm or more. These animals "loosen" the sedimentary fabric, increase the water content in the sediment, thereby lowering the sediment shear strength, and actively recycle nutrients because of the high exchange rate with the overlying waters resulting from their burrowing and feeding activities.

In dynamic estuarine and coastal environments, it is simplistic to assume that benthic communities always progress completely and sequentially through all four stages in accordance with the idealized conceptual model depicted in Figure 4. Various combinations of these basic successional stages are possible. For example, secondary succession can occur (Horn, 1974) in response to additional labile carbon input to surface sediments, with surface-dwelling Stage 1 or 2 organisms co-existing at the same time and place with Stage 3, resulting in the assignment of a "Stage 1 on 3" or "Stage 2 on 3" designation.

While the successional dynamics of invertebrate communities in fine-grained sediments have been well-documented, the successional dynamics of invertebrate communities in sand and coarser sediments are not well-known. Subsequently, the insights gained from sediment profile imaging technology regarding biological community structure and dynamics in sandy and coarse-grained bottoms are fairly limited.

2.1.5 Biological Mixing Depth

During the past two decades, there has been a considerable emphasis on studying the effects of bioturbation on sediment geotechnical properties as well as sediment diagenesis (Ekman et al., 1981; Nowell et al., 1981; Rhoads and Boyer, 1982; Grant et al., 1982; Boudreau, 1986; 1994; 1998). However, an increasing focus of research is centering on the rates of contaminant flux in sediments (Reible and Thibodeaux, 1999; François et al., 2002; Gilbert et al., 2003), and the two parameters that affect the time rate of contaminant flux the greatest are erosion and bioturbation (Reible and Thibodeaux, 1999). The depth to which sediments are bioturbated, or the biological mixing depth, can be an important parameter for studying either nutrient or contaminant flux in sediments. While the apparent RPD is one potential measure of biological mixing depth, it is quite common in profile images to see evidence of biological activity (burrows, voids, or actual animals) well below the mean apparent RPD. Both the minimum and maximum linear distance from the sediment surface to both the shallowest and deepest feature of biological activity can be measured along with a notation of the type of biogenic structure measured. For this report, the maximum depth to which any biological activity was noted was measured and mapped.

.

3.0
RESULTS

While replicate images were taken at each station, the amount of disturbance caused by the diver-deployed system did not allow for reliable measurements of precision between the two replicate images, so only one replicate (the least disturbed) from each station sampled by divers was analyzed. The amount of debris in and around the piers coupled with the high density of shell fragments also created high variation in the penetration depth at the frame deployed stations, with cross-sectional sedimentary structures masked or destroyed by debris (natural or anthropogenic) being dragged down by the prism cutting blade. While a copy of all images collected was provided to the client, given the variation in image feature preservation (regardless of whether they were taken with the frame-deployed or diver-deployed system), and because this variation in cross-sectional structural appearance was not really indicative of natural variance in the measured parameters, the best image (least disturbed) from each station was analyzed. A complete set of all the summary data measured from each image is presented in Appendix A.

The results for some SPI parameters are sometimes indicated in the data appendix or on the maps as being "Indeterminate" (Ind). This is a result of the sediments being either: 1) too compact for the profile camera to penetrate adequately, preventing observation of surface or subsurface sediment features, 2) too soft to bear the weight of the camera, resulting in over-penetration to the point where the sediment/water interface was above the window (imaging area) on the camera prism (the sediment/water interface must be visible to measure most of the key SPI parameters like aRPD depth, penetration depth, and infaunal successional stage), or 3) the biogenic and sedimentary stratigraphic structure was compromised or destroyed by sampling artifacts caused by the divers inserting the prism into the sediment (either vibrating or wiggling the camera to achieve greater penetration, which allowed suspended sediment to collect in between the cross-sectional profile and the faceplate of the prism)

Although there are some uncertainties associated with SPI data as discussed above, the technology has been shown to be a powerful reconnaissance tool that can efficiently map gradients in sediment type, biological communities, or disturbances from physical forces or organic enrichment. The results and conclusions in this report are about dynamic processes that have been deduced from imaged structures; as such, they should be considered hypotheses available for further testing/confirmation.

3.1 PRISM PENETRATION DEPTH

Sediments throughout the site ranged from sandy silt to muds with minor fractions of very fine to fine sand with high percentages of shell hash (stations under Pier 7; see Figure 5) to pebble and cobble armoring over silty sands (Figure 6). As noted from the results of the past two surveys, the addition of the AquaGate amendment also provided some surface armoring at select stations which impeded camera prism penetration (Figure 7). The overall site prism penetration depth was similar to the values measured in 2013 (T = 10 months), with values ranging from 2.3 to 20.0 cm, with an overall site average of 12.2 cm; the spatial distribution of mean penetration depth at all stations sampled is shown in Figure 8.

3.2 THICKNESS OF REACTIVE AMENDMENT LAYER

Measureable deposits of AquaGate+PAC^{TM} could be seen at 14 stations this year as compared to 16 stations last year; natural depositional processes and bioturbation of the sediments by the resident infauna will mask the signature of this depositional layer over time. At those stations where the cap material could be detected, the mean thickness ranged from trace layers to 18.6 cm, with an average thickness of 10.5 cm at those 14 stations where a distinct layer could be measured. The footprint of the visible cap is shown in Figure 9.

3.3 APPARENT REDOX POTENTIAL DISCONTINUITY DEPTH

The distribution of mean apparent RPD depths is shown in Figure 10; mean aRPD depths could not be measured at 5 of the stations sampled by divers because of sampling artifacts that caused distortions to the sediment profile and eliminated the possibility of any accurate measurements; cobble/shell or drag-down of surface megafauna (serpulid polychaetes or anemones) at 5 of the stations sampled with the frame camera either prevented sufficient prism penetration (cobble/shell stations) or distorted the structure of the sediment profile against the faceplate (faunal interference) to prevent measurement of an accurate aRPD measurement. While one station still had no detectable aRPD present (compared with 8 stations in 2013), the remaining stations had values ranging from 0.2 to 5.9 cm (Figure 10; Appendix A), with an overall site average of 2.1 cm.

3.4 INFAUNAL SUCCESSIONAL STAGE

The mapped distribution of infaunal successional stages is shown in Figure 11; there was a noticeable improvement in biological community status under the pier as well as at the stations outboard of the pier compared with 2013 (T = 10 months). There were 8 stations where either prism penetration was too shallow or the profile was disturbed by sampling

artifacts where infaunal successional status could not be determined, and there was one station under the pier (Figure 12) where there were retrograde habitat conditions compared to 2013 (Station 6-2). However, the presence of Stage 3 taxa (larger infaunal deposit feeders) was evident at 34 of the 50 stations (compared to only 18 stations in 2013 where Stage 3 taxa were evident).

3.5 MAXIMUM BIOLOGICAL MIXING DEPTH

The spatial distribution of the maximum depth to which any biological activity was seen in the study area is shown in Figure 13. Some of the deepest infaunal burrowing was found at those stations under the pier where the reactive amendment had been placed; maximum depth of biogenic activity ranged from 4.7 to 20.2 cm, with an overall site average of 12.1 cm.

4.0
DISCUSSION

The results from this third post-capping SPI survey showed gradual improvement and recovery following the disturbance of the capping operation, as predicted by soft-bottom successional research (Figure 4). Over time and with the lack of continued severe disturbance, the appearance of Stage 3 (deposit-feeding) taxa as part of the resident infauna are not only re-working the reactive amendment into the sediment but also causing the depth of the aRPD to increase (Figure 14) as well fostering increased nutrient exchange with the overlying water.

The pattern of the optical signature of the reactive amendment slowly "disappearing" through natural depositional processes and bioturbational activity of the infaunal community that was documented in the 2013 survey continued in this survey; initially, the presence of the reactive amendment could be detected at 19 stations. After 10 months post placement (2013 survey), the layer was only visible at 16 stations, and in this most recent survey (22 months post placement), the layer could only be detected at 14 stations (Figure 9).

While this survey showed that the activated cap amendment continues to be reworked into the sediments by the resident infauna as originally planned and overall habitat quality appears to be gradually improving over time , there was one location under the pier where this was not the case. Station 6/5-2 continues to look the same as it did right after the material was placed in 2012 and as it did in the 2013 survey (Figure 15); there was no detectable aRPD and a notable lack of deposit-feeding taxa from more mature infaunal successional assemblages. It could be that sediments in this one small area are still chemically-challenged and inhibiting successful recolonization by native infauna.

None of this work would have been possible without the cooperation and hard work by the PSNS & IMF Bremerton site divers. We would like to acknowledge both their attention to safety and skill in sample collection; it was truly a pleasure to have been able to collaborate with them and the rest of the PSNS & IMF Bremerton site personnel on this project over the past few years.

5.0
REFERENCES CITED

Boudreau, B.P. 1986. Mathematics of tracer mixing in sediment. I-Spatially-dependent, diffusive mixing. II: Non-local mixing and biological conveyor-belt phenomena. Am. Jour. Sci. 286: 161-238.

Boudreau, B.P. 1994. Is burial velocity a master parameter for bioturbation? Geochimica et Cosmochemica Acta 58: 1243-1249.

Boudreau, B. P. 1998. Mean mixed depth of sediments: The wherefore and the why. Limnol. Oceanogr. 43: 524-526.

Diaz, R. J. and L. C. Schaffner. 1988. Comparison of sediment landscapes in the Chesapeake Bay as seen by surface and profile imaging, p. 222-240 In M. P. Lynch and E. C. Krome (eds.), Understanding the Estuary: Advances in Chesapeake Bay Research, Chesapeake Bay Research Consortium Publication 129, Chesapeake Bay Program 24/88.

Ekman, J.E., Nowell, A.R.M., and P.A. Jumars. 1981. Sediment destabilization by animal tubes. J. Mar. Res. 39: 361-374.

Fenchel, T. 1969. The ecology of marine macrobenthos IV. Structure and function of the benthic ecosystem, its chemical and physical factors and the microfauna communities with special reference to the ciliated protozoa. Ophelia 6: 1-182.

François, F., Gerino, M., Stora, G., Durbec, J.P., and J.C. Poggiale. 2002. Functional approach to sediment reworking by gallery-forming macrobenthic organisms: modeling and application with the polychaete *Nereis diversicolor*. Marine Ecology Progress Series 229: 127–136.

Fredette, T.J., W.F. Bohlen, D.C. Rhoads, and R.W. Morton. 1988. Erosion and resuspension effects of Hurricane Gloria at Long Island Sound dredged material disposal sites. In: Proceedings of the Water Quality ‘88 seminar, February Meeting, Charleston, South Carolina. U.S. Army Corps of Engineers, Hydraulic Engineering Center, Davis, CA.

Germano, J.D. 1983. Infaunal succession in Long Island Sound: Animal-sediment interactions and the effects of predation. Ph.D. dissertation. Yale University, New Haven, CT. 206 pp.

Germano & Associates, Inc., (G&A) 2013a. Sediment Profile Imaging Report Demonstration of in-situ Treatment of Contaminated Sediments With Reactive Amendments: Baseline Survey. Germano & Associates Bellevue, WA, March 2013, 35pp.

Germano & Associates, Inc., 2013b. Sediment Profile Imaging Report Demonstration of in-situ Treatment of Contaminated Sediments With Reactive Amendments: Post Cap Survey #1. Germano & Associates Bellevue, WA, March 2013, 41pp.

Germano & Associates, Inc., 2014. Sediment Profile Imaging Report Demonstration of in-situ Treatment of Contaminated Sediments with Reactive Amendments: Post Cap Survey #2. Germano & Associates Bellevue, WA, January 2014, 44pp.

Germano, J.D. and D.C. Rhoads. 1984. REMOTS sediment profiling at the Field Verification Program (FVP) Disposal Site. In: Dredging '84 Proceedings, ASCE, Nov. 14-16, Clearwater, FL. pp. 536-544.

Germano, J.D., D.C. Rhoads, R.M. Valente, D.A. Carey, and M. Solan. 2011. The use of Sediment Profile Imaging (SPI) for environmental impact assessments and monitoring studies – lessons learned from the past four decades. Oceanography and Marine Biology: An Annual Review 49: 247-310.

Gilbert, F. S. Hulth, N. Strömberg, K. Ringdahl, and J.-C. Poggiale. 2003. 2-D optical quantification of particle reworking activities in marine surface sediments. Jour. Exp. Mar. Biol. Ecol. 285-286: 251-264.

Grant, W.D., Jr., Boyer, L.F., and Sanford, L.P. 1982. The effects of bioturbation on the initiation of motion of intertidal sands: Jour. Mar. Res., Vol. 40, pp. 659-677.

Horn, H.S. 1974. The ecology of secondary succession. Ann. Rev. Ecol. Syst. 5: 25-37.

Huettel, M., Ziebis, W., Forster., S., and G.W. Luther III. 1998. Advective transport affecting metal and nutrient distributions and interfacial fluxes in permeable sediments. Geochimica et Cosmochemica Acta 62: 613-631.

Johnston, R.K., V. Kirtay, D.B. Chadwick, G.H. Rosen, J.M. Guerrero, J. Collins, C. Ortega, R. Webb, R,. May, J. Germano, D. Browning, E. Beaver, M. Wicklein, J. Pittz, D.E. Leisle, L. Doyle, and L. Hsu. 2013. Installing an activated-carbon sediment amendment at the Puget Sound Naval Shipyard and Intermediate Maintenance Facility, Bremerton, WA. Paper B-024, Proceedings of the Seventh International Conference on Remediation of Contaminated Sediments (Dallas, TX; February 4-7, 2013). ISBN 978-0-9818730-6-7. ©2013 Battelle Memorial Institute, Columbus, OH. www.battelle.org/sedimentscon

Lyle, M. 1983. The brown-green colour transition in marine sediments: A marker of the Fe (III) – Fe(II) redox boundary. Limnol. Oceanogr. 28: 1026-1033.

Nowell, A.R.M., P.A. Jumars, and J.E. Ekman. 1981. Effects of biological activity on the entrainment of marine sediments. Mar. Geol. 42: 133-153.

Painter, T.H., M. E. Schaepman, W. Schweizer, and J. Brazile. 2007. Spectroscopic discrimination of shit from shinola. Annals of Improbable Research 13: 22-23.

Pearson, T.H. and R. Rosenberg. 1978. Macrobenthic succession in relation to organic enrichment and pollution of the marine environment. Oceanogr. Mar. Biol. Ann. Rev. 16:229-311.

Reible, D and Thibodeaux, L. 1999. Using Natural Processes to Define Exposure From Sediments., in Sediment Management Work Group; Contaminated Sediment Management Technical Papers, Sediment Management Work Group, http://www.smwg.org/index.htm.

Revelas, E.C., J.D. Germano, and D.C. Rhoads. 1987. REMOTS reconnaissance of benthic environments. pp. 2069-2083. In: Coastal Zone '87 Proceedings, ASCE, WW Division, May 26-29, Seattle, WA.

Rhoads, D.C. 1974. Organism-sediment relations on the muddy seafloor. Oceanogr. Mar. Biol. Ann. Rev. 12: 263-300.

Rhoads, D.C. and L.F. Boyer. 1982. The effects of marine benthos on physical properties of sediments. pp. 3-52. In: Animal-Sediment Relations. McCall, P.L. and M.J.S. Tevesz (eds). Plenum Press, New York, NY.

Rhoads, D.C. and J.D. Germano. 1982. Characterization of benthic processes using sediment profile imaging: An efficient method of remote ecological monitoring of the seafloor (REMOTS™ System). Mar. Ecol. Prog. Ser. 8:115-128.

Rhoads, D.C. and J.D. Germano. 1986. Interpreting long-term changes in benthic community structure: A new protocol. Hydrobiologia. 142:291-308.

Rhoads, D.C. and J.D. Germano. 1990. The use of REMOTS® imaging technology for disposal site selection and monitoring. pp. 50-64. In: Geotechnical Engineering of Ocean Waste Disposal, K. Demars and R. Chaney (eds). ASTM Symposium Volume, January, 1989. Orlando, FL.

Rosenberg, R., H.C. Nilsson, and R.J. Diaz. 2001. Response of benthic fauna and changing sediment redox profiles over a hypoxic gradient. Estuarine, Coastal and Shelf Science 53: 343-350.

Valente, R.M., D.C. Rhoads, J.D. Germano, and V.J. Cabelli. 1992. Mapping of benthic enrichment patterns in Narragansett Bay, RI. Estuaries 15:1-17.

Ziebis, W., Huettel, M., and S. Forster. 1996. Impact of biogenic sediment topography on oxygen fluxes in permeable seabeds. Mar. Ecol. Prog. Ser. 140: 227-237.

FIGURES

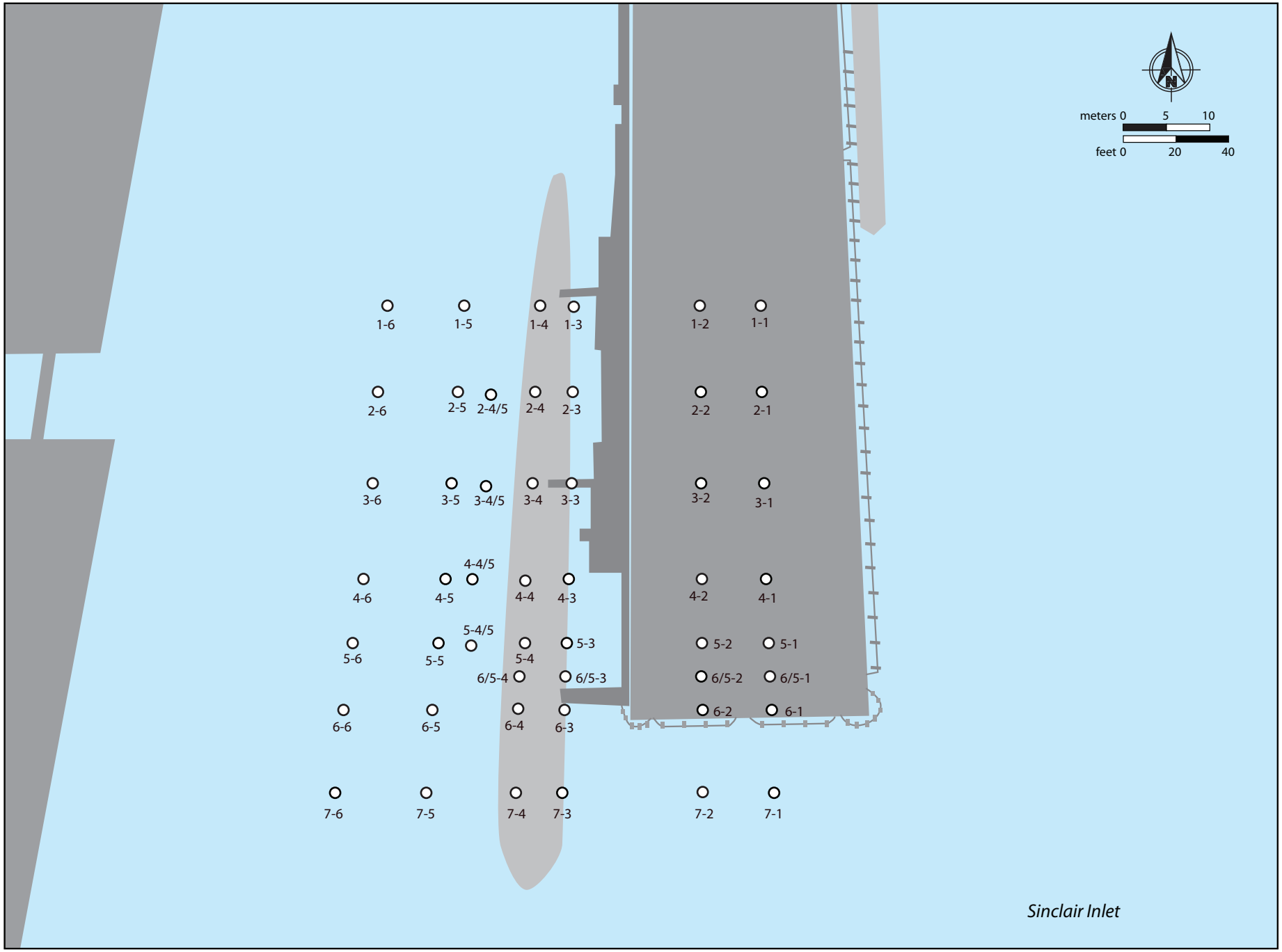

Figure 1: Location of SPI stations under and around Pier 7 at PSNS & IMF, Bremerton site, that were monitored in August 2013 and July 2014.

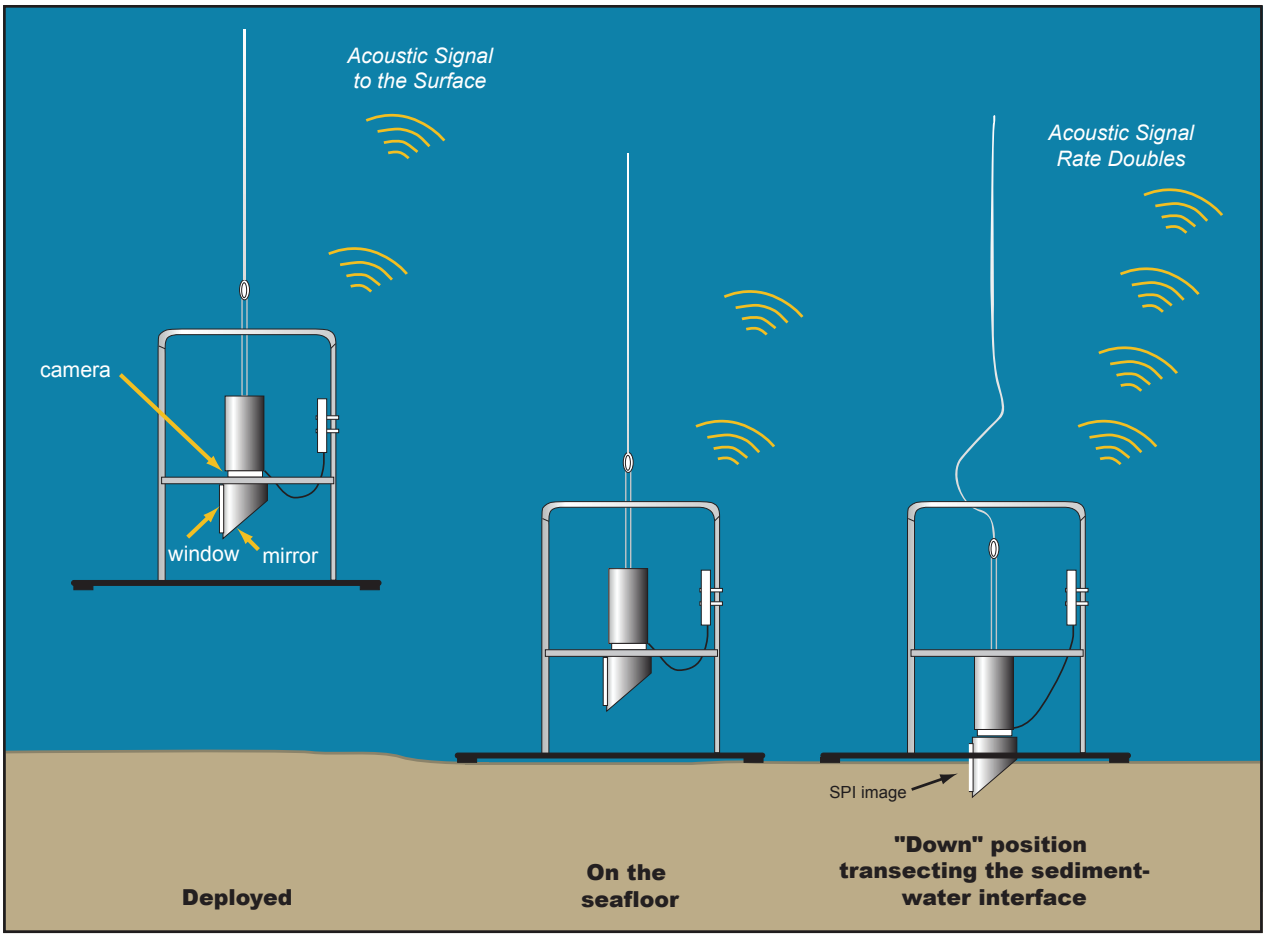

Figure 2: Deployment and operation of the SPI camera system.

Figure 3: The hand-held SPI system used by divers for all stations that were located underneath Pier 7 at PSNS & IMF, Bremerton site.

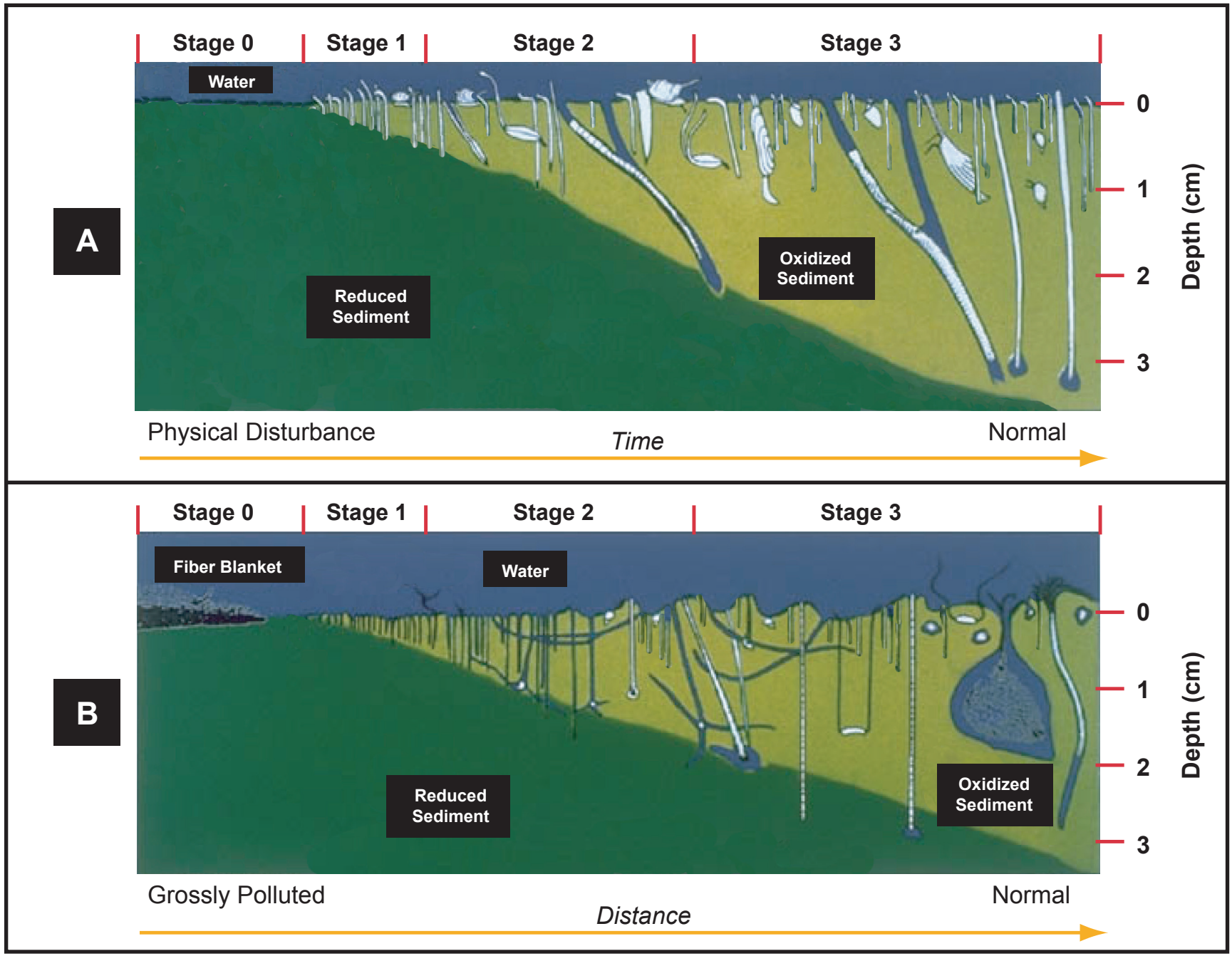

Figure 4: The stages of infaunal succession as a response of soft-bottom benthic communities to physical disturbance (top panel) or organic enrichment (bottom panel). From Rhoads and Germano, 1982.

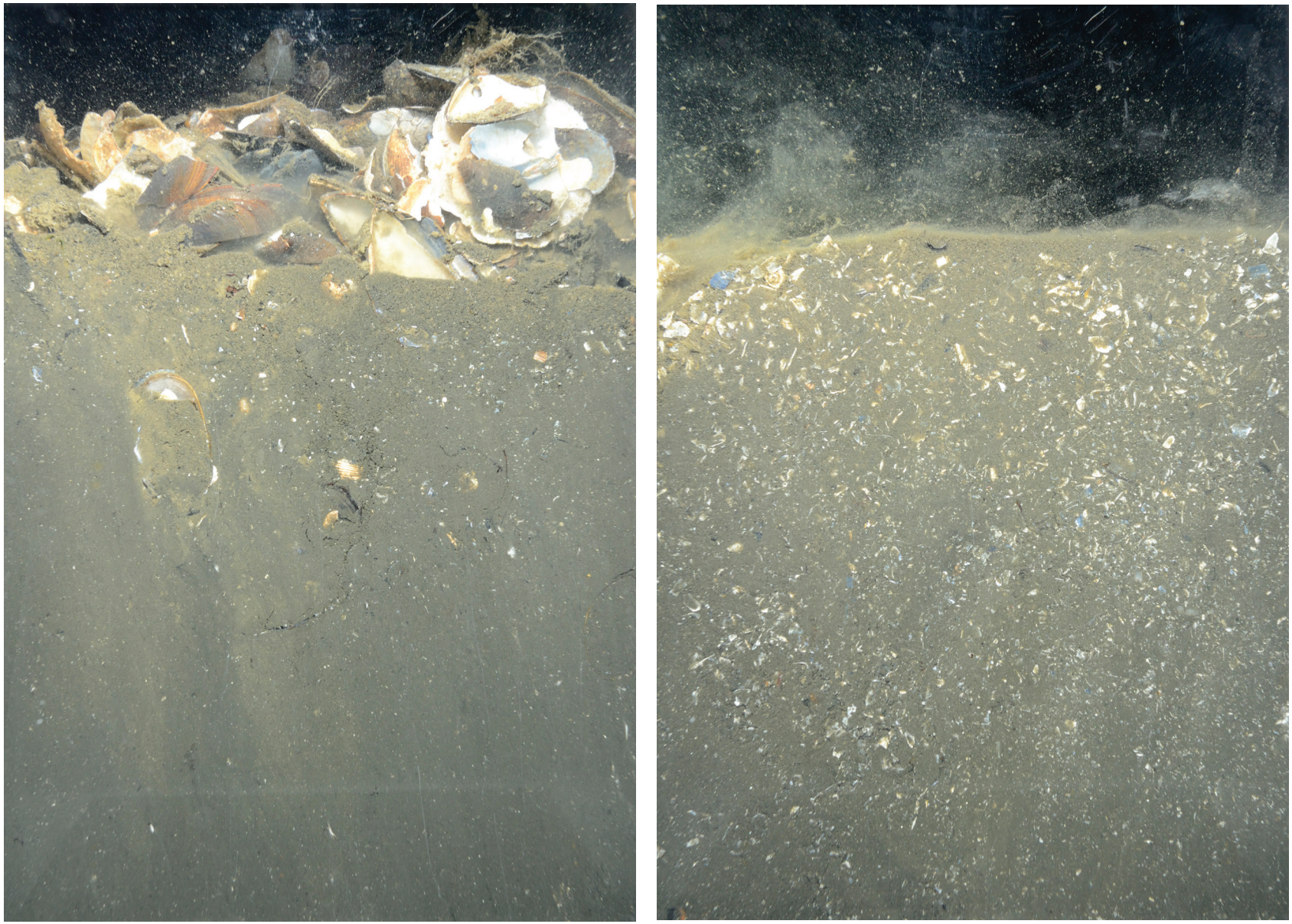

1-2 5-1

Figure 5: These profile images from Station 1-2 and Station 5-1 show the different forms of surface armoring from shell hash (intact shells at Station 1-2 versus pulverized fragments at Station 5-1) found at many of the under pier stations. Scale: width of each profile image = 14.5 cm.

Figure 6: As in past surveys, the SPI photos from Station 1-3 show an armoring of pebble and cobbles over silty very fine sand. Scale: width of profile image = 14.5 cm.

Figure 7: This profile image from Station 5-3 shows surface armoring from the pebbles used as a carrier vehicle for the activated carbon in the AquaGate amendment that was placed under and around Pier 7. Scale: width of profile image = 14.5 cm.

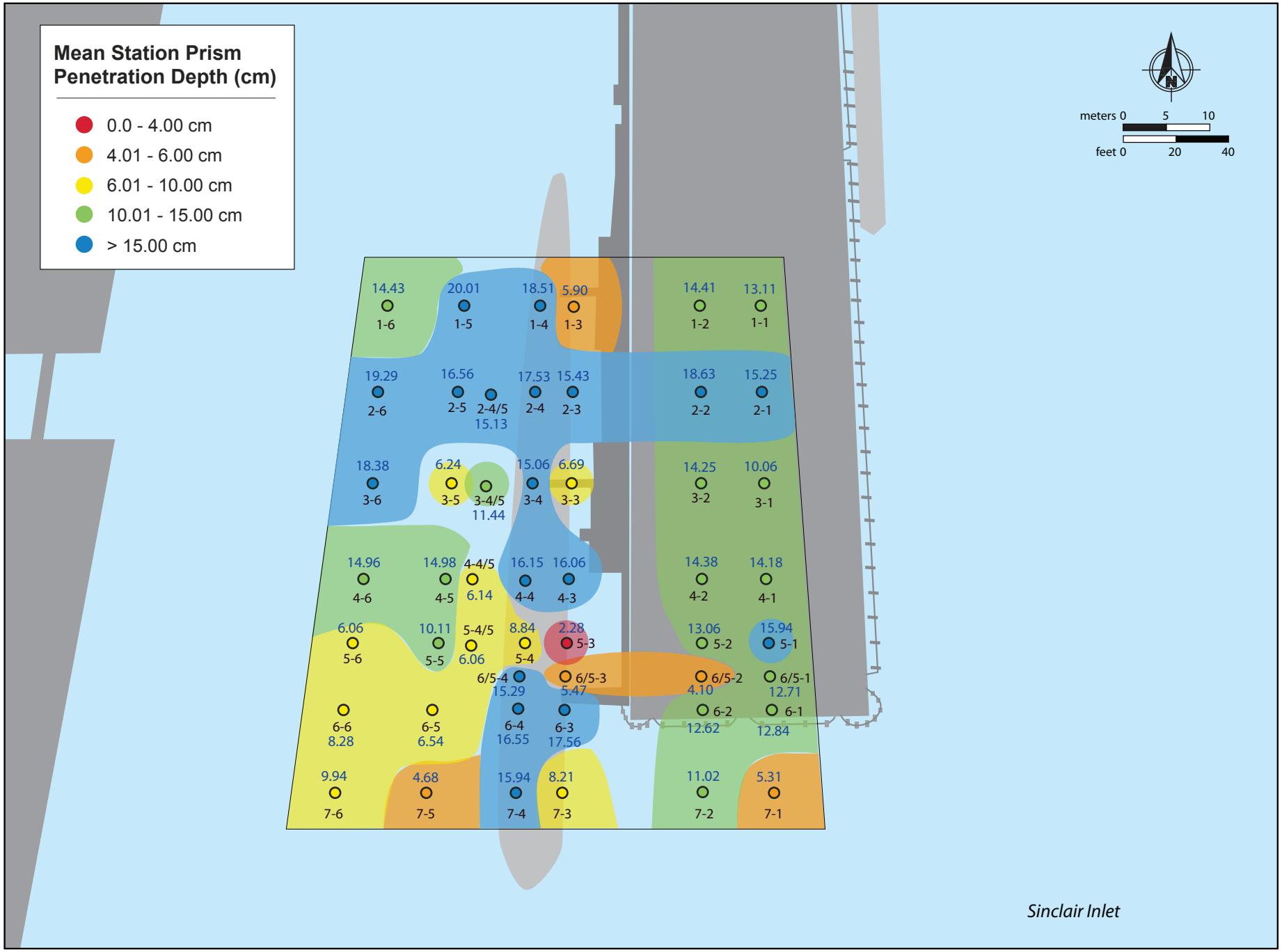

Figure 8: Spatial distribution of mean camera prism penetration depth (cm) at Pier 7 at the PSNS & IMF Bremerton site in July 2014.

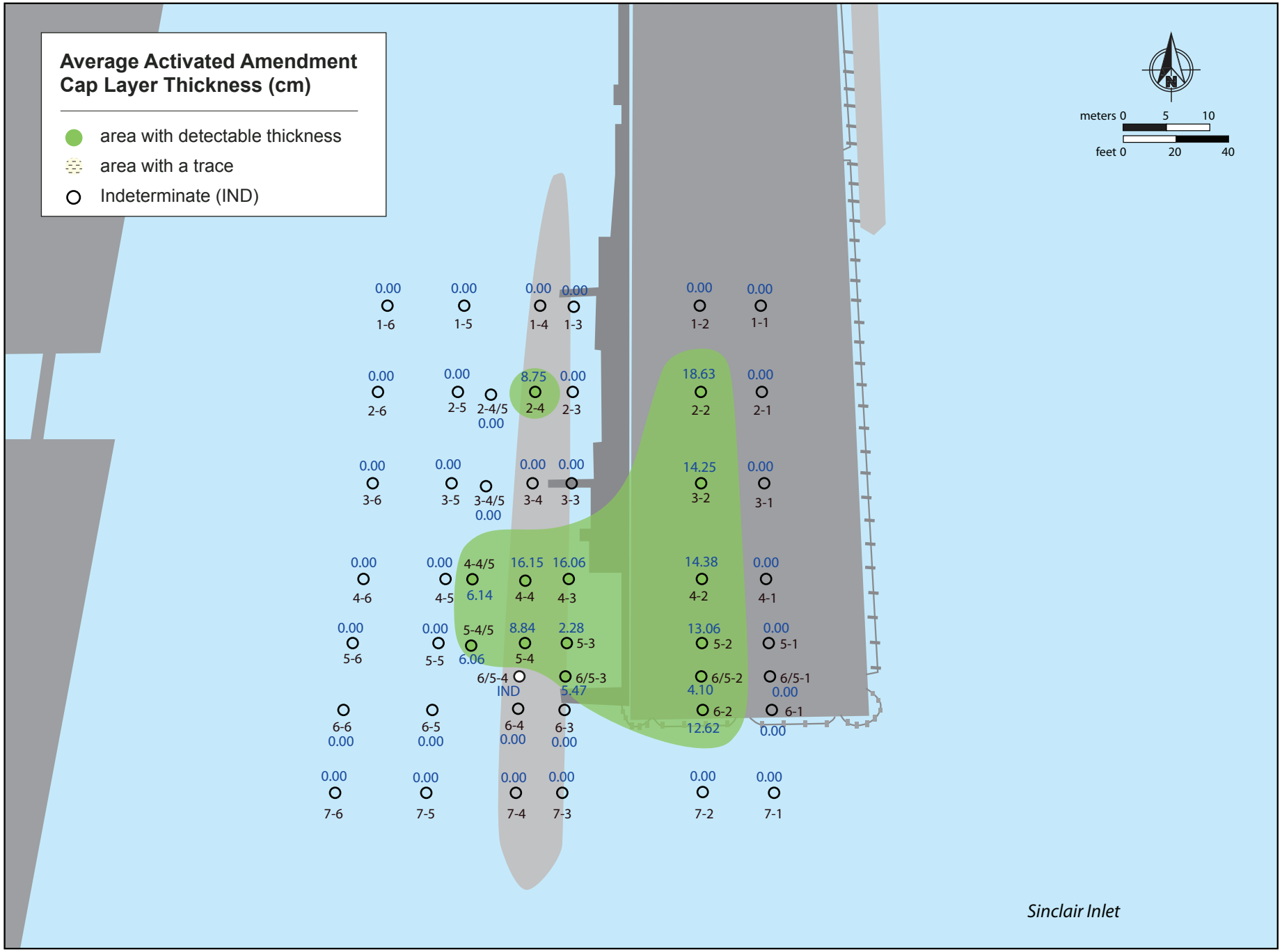

Figure 9: Spatial distribution and mean depositional thickness (cm) of the AquaGate +PAC™ material placed at locations in and around Pier 7 at the PSNS & IMF Bremerton site.

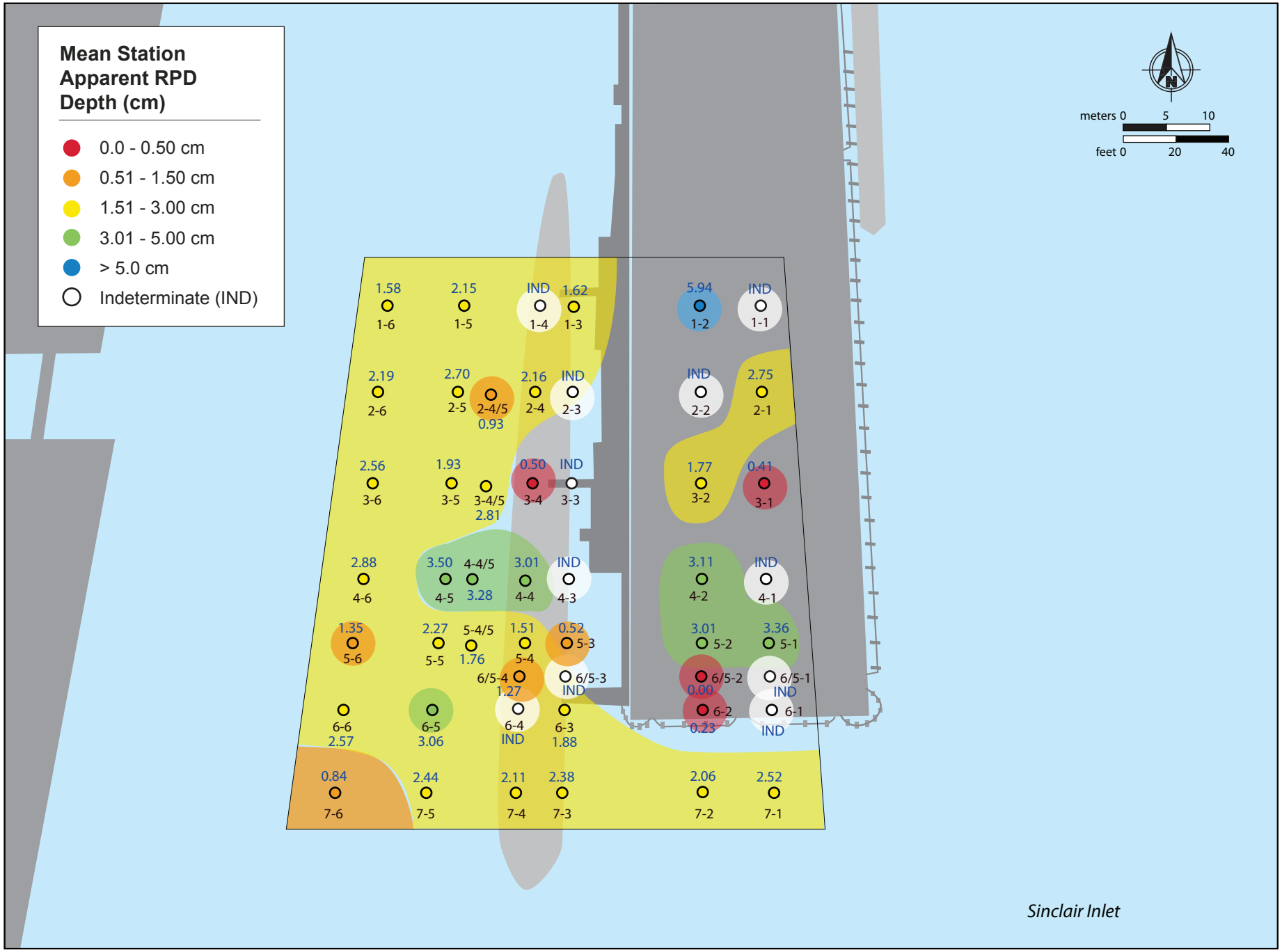

Figure 10: Spatial distribution of mean aRPD depth (cm) at Pier 7 at the PSNS & IMF Bremerton site in July 2014.

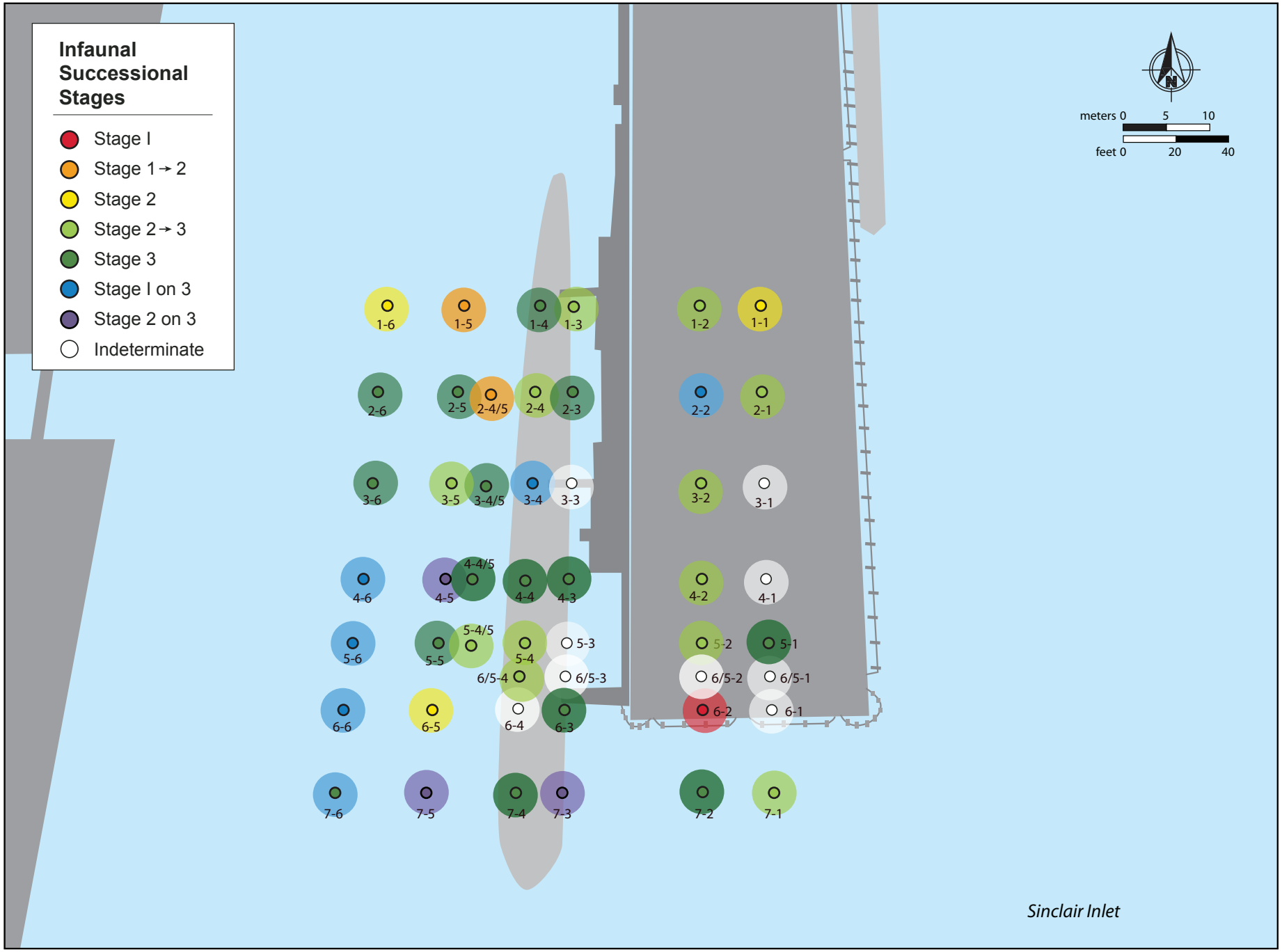

Figure 11: Spatial distribution of infaunal successional stages at Pier 7 at the PSNS & IMF Bremerton site in July 2014.

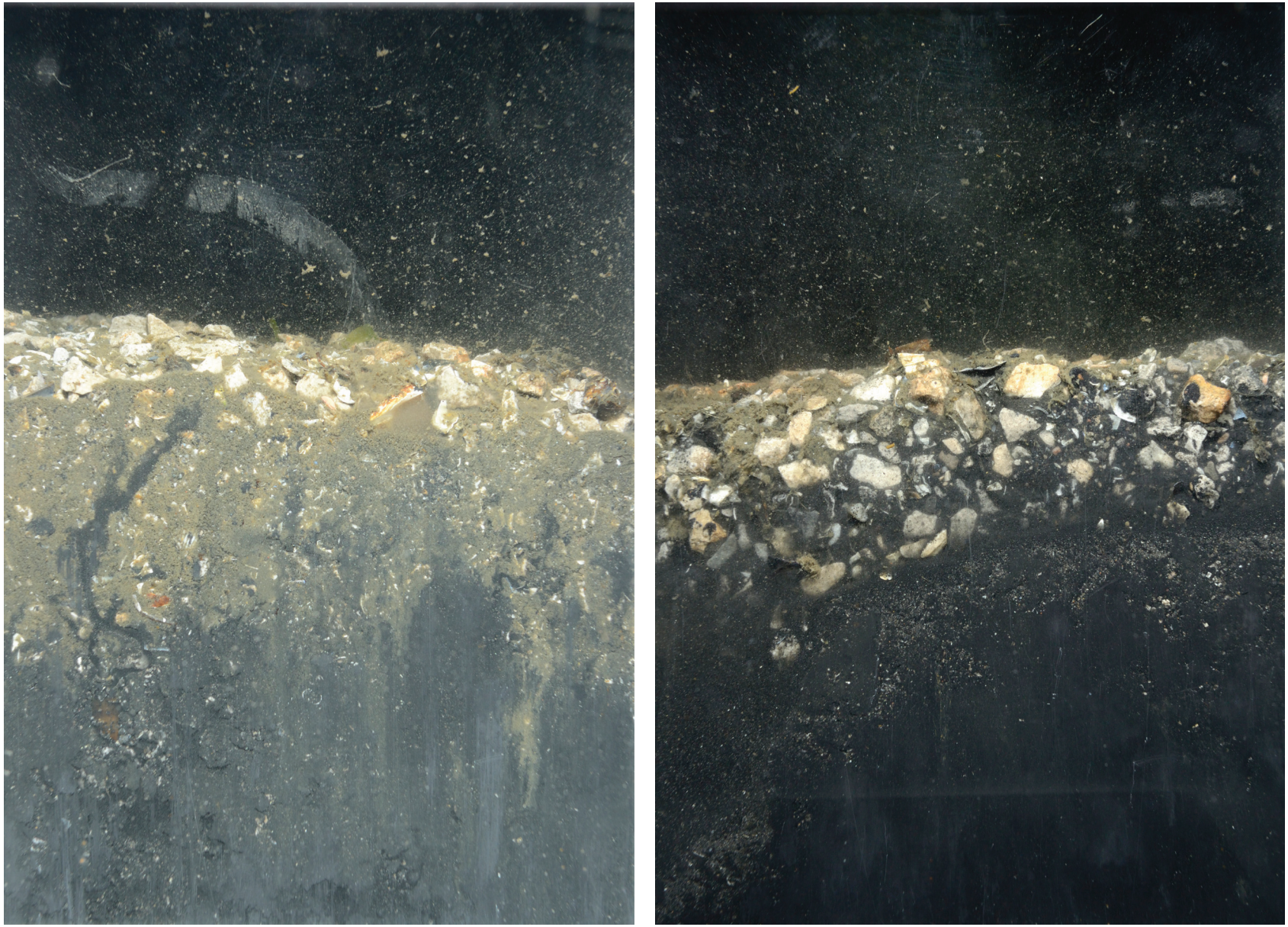

2013: 6-2 **2014: 6-2**

Figure 12: These profile images from Station 6-2 from 2013 (left) and 2014 (right) show a degradation in habitat conditions for the benthic infaunal community. Scale: width of each profile image = 14.5 cm.

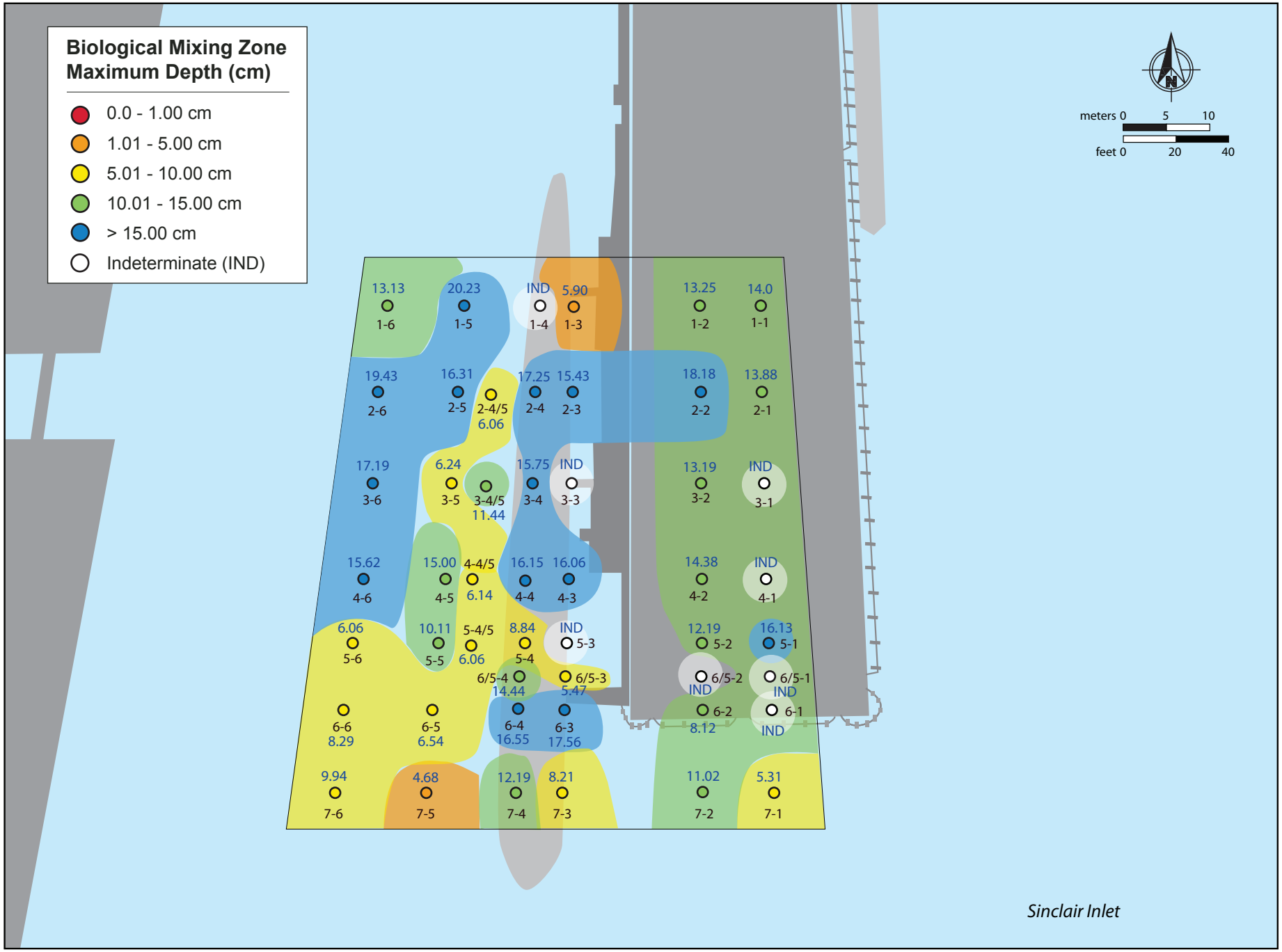

Figure 13: Spatial distribution of maximum biological mixing depth (cm) at Pier 7 at the PSNS & IMF Bremerton site in July 2014.

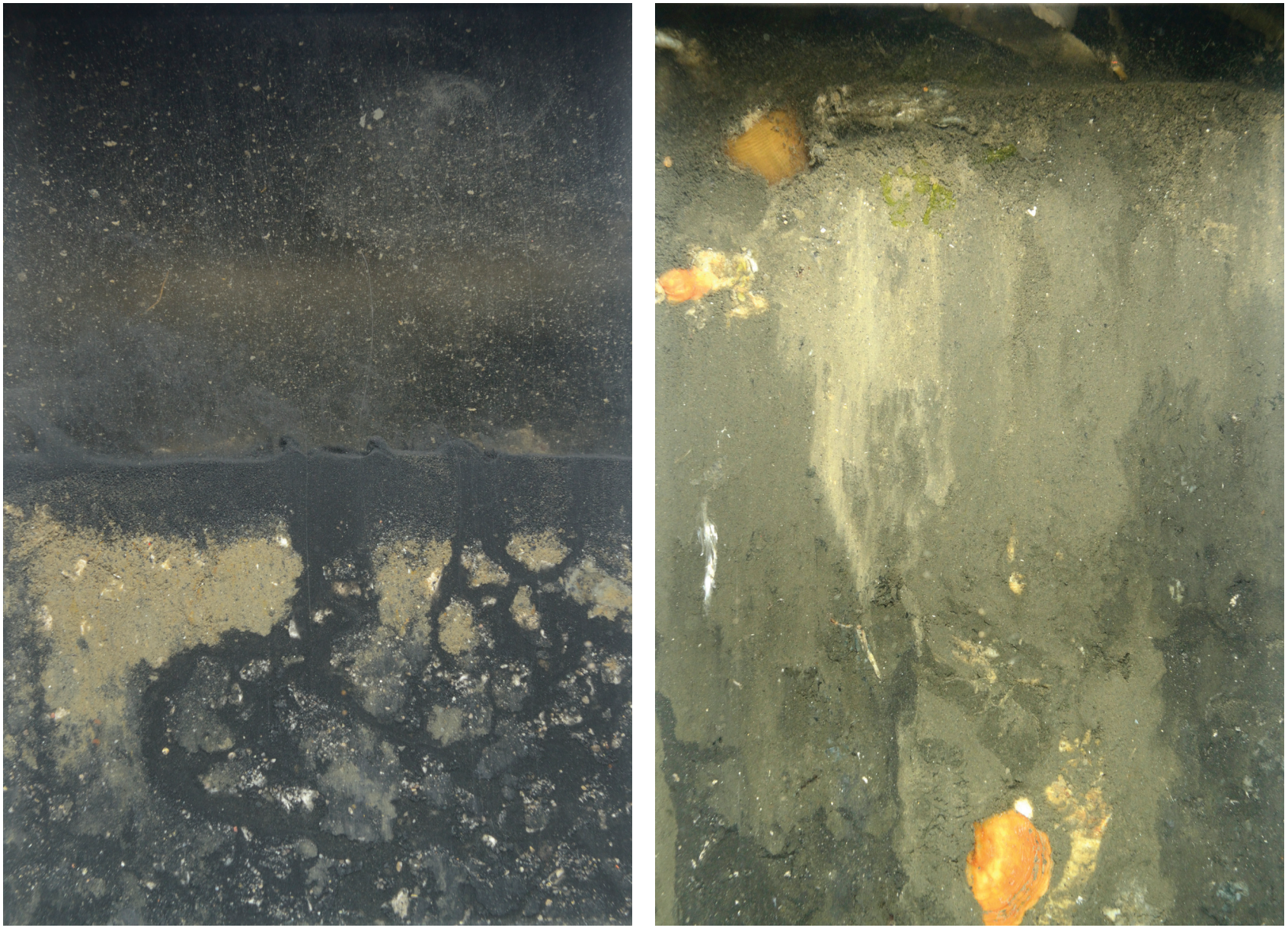

2013: 4-4 **2014: 4-4**

Figure 14: These profile images from Station 4-4 from 2013 (left) and 2014 (right) show the progression of normal infaunal successional recovery over time as predicted by previous research in soft bottom recolonization studies. Scale: width of each profile image = 14.5 cm.

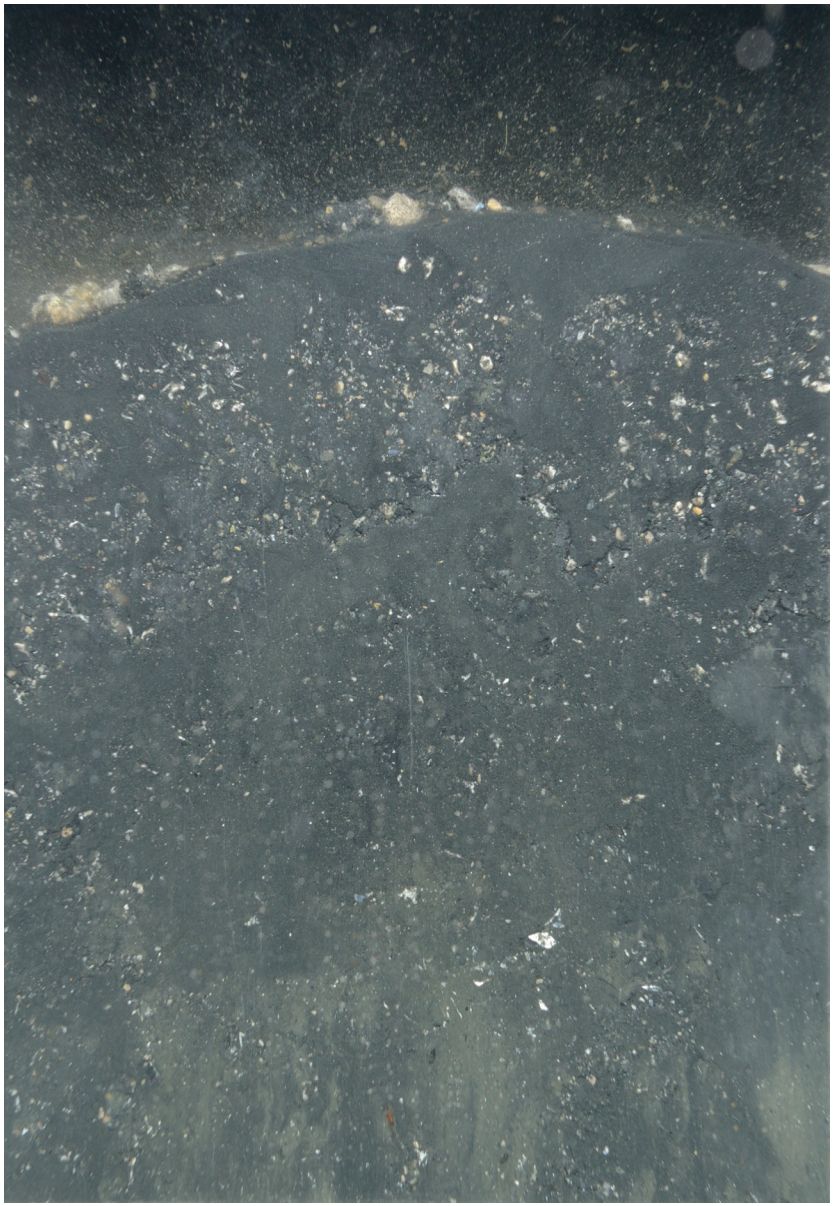

2013: 6/5-4

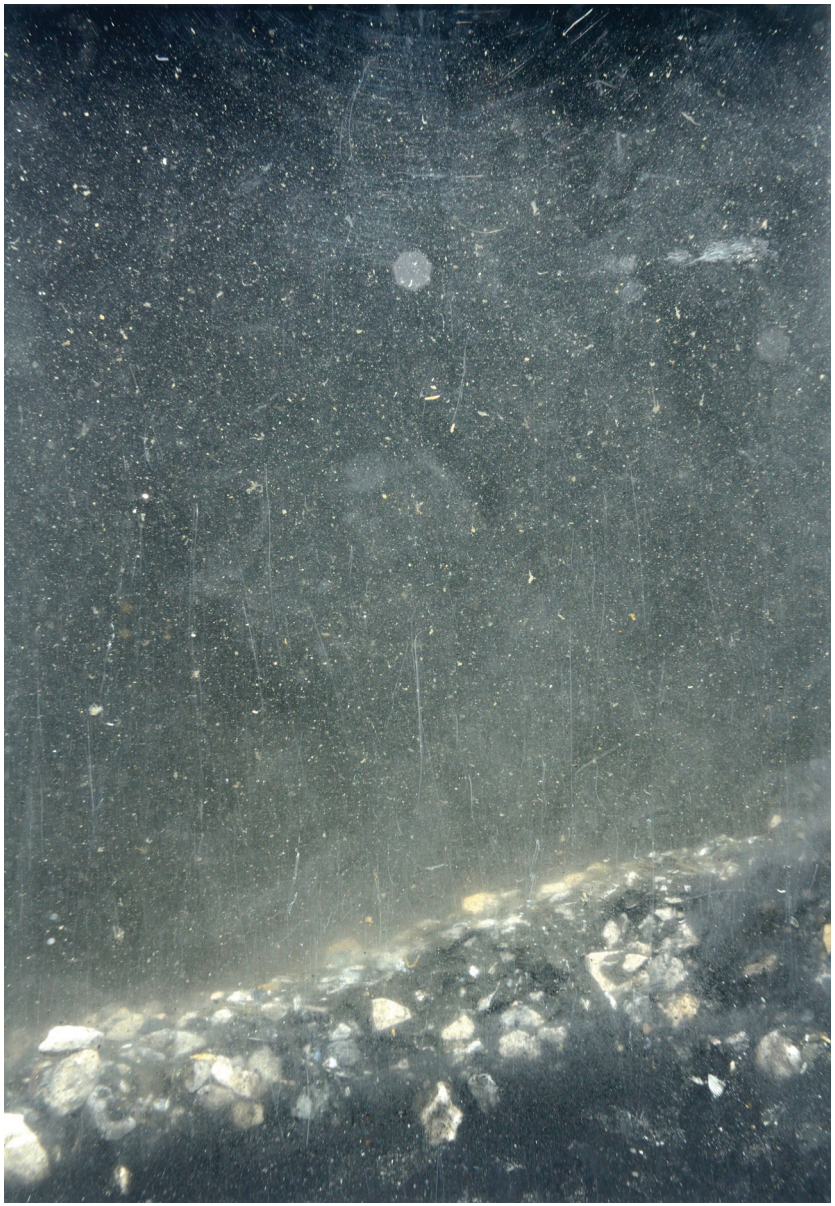

2014: 6/5-4

Figure 15: These profile images from Station 6/5-2 from 2013 (left) and 2014 (right) reveal little progress in infaunal community development even 2 years after the reactive amendment was placed in contrast to all the other locations. Scale: width of each profile image = 14.5 cm.

APPENDIX A

Sediment Profile Image Analysis Results

Station	Replicate	Date	Time	Stop Collar Setting (in)	# of Weights (per side)	Calibration Constant	Penetration Mean (cm)	RPD Area (sq.cm)	Mean RPD (cm)	GAC depth (cm)	Mixing Zone Max Depth (cm)	Succes sional Stage
1-1	B	7/29/2014	12:33:50	NA	NA	14.52	13.11	Ind	Ind	0.00	14.0	2
1-2	A	7/29/2014	12:22:05	NA	NA	14.52	14.41	86.21	5.94	0.00	13.25	2 -> 3
1-3	A	7/30/2014	13:40:34	15	4	14.52	5.90	23.51	1.62	0.00	5.90	2 -> 3
1-4	C	7/30/2014	13:50:52	15	4	14.52	18.51	Ind	Ind	0.00	ind	3
1-5	C	7/30/2014	13:23:28	15	4	14.52	20.01	31.16	2.15	0.00	20.23	1->2
1-6	A	7/30/2014	13:13:45	15	4	14.52	14.43	23.00	1.58	0.00	13.13	2
2-1	A	7/29/2014	12:05:14	NA	NA	14.52	15.25	39.93	2.75	0.00	13.88	2 -> 3
2-2	B	7/29/2014	11:58:55	NA	NA	14.52	18.63	Ind	Ind	18.63	18.18	1 on 3
2-3	A	7/30/2014	14:35:08	15	4	14.52	15.43	0.00	Ind	Ind	15.43	3
2-4	B	7/30/2014	14:40:37	15	4	14.52	17.53	31.40	2.16	8.75	17.25	2 -> 3
2-5	B	7/30/2014	14:14:52	15	4	14.52	16..56	39.19	2.70	0.00	16.31	**3**
2-6	A	7/30/2014	14:08:12	15	4	14.52	19.29	31.76	2.19	0.00	19.43	3
3-1	A	7/29/2014	11:03:02	NA	NA	14.52	10.06	5.98	0.41	0.00	ind	Ind
3-2	B	7/29/2014	10:58:50	NA	NA	14.52	14.25	25.67	1.77	14.25	13.19	2 -> 3
3-3	C	7/30/2014	12:39:20	15	4	14.52	6.69	Ind	Ind	0.00	ind	Ind
3-4	A	7/30/2014	12:44:47	15	4	14.52	15.06	7.30	0.50	0.00	15.75	1 on 3
3-5	C	7/30/2014	12:19:51	15	4	14.52	6.24	28.13	1.93	0.00	6.24	2 -> 3
3-6	C	7/30/2014	12:25:21	15	4	14.52	18.38	37.21	2.56	0.00	17.19	3
4-1	B	7/29/2014	10:47:45	NA	NA	14.52	14.18	Ind	Ind	0.00	ind	Ind
4-2	A	7/29/2014	10:38:37	NA	NA	14.52	14.38	45.17	3.11	14.38	14.38	2 -> 3
4-3	A	7/30/2014	10:25:39	15	4	14.52	16.06	Ind	Ind	16.06	16.06	3
4-4	C	7/30/2014	10:31:35	15	4	14.52	16.15	Ind	3.01	16.15	16.15	3
4-5	B	7/30/2014	11:09:49	15	4	14.52	14.98	50.82	3.50	0.00	15.00	2 on 3
4-6	A	7/30/2014	11:15:15	15	4	14.52	14.96	41.75	2.88	0.00	15.62	1 on 3
5-1	B	7/29/2014	10:29:19	NA	NA	14.52	15.94	48.71	3.36	0.00	16.13	3
5-2	A	7/29/2014	10:18:33	NA	NA	14.52	13.06	43.67	3.01	13.06	12.19	2 -> 3

Station	Replicate	Date	Time	Stop Collar Setting (in)	# of Weights (per side)	Calibration Constant	Penetration Mean (cm)	RPD Area (sq.cm)	Mean RPD (cm)	GAC depth (cm)	Mixing Zone Max Depth (cm)	Succes sional Stage
5-3	A	7/30/2014	10:43:14	15	4	14.52	2.28	7.53	0.52	2.28	ind	Ind
5-4	A	7/30/2014	8:30:15	16	4	14.52	8.84	21.85	1.51	8.84	8.84	2 -> 3
5-5	B	7/30/2014	9:51:56	15	4	14.52	10.11	33.00	2.27	0.00	10.11	3
5-6	C	7/30/2014	9:49:08	15	4	14.52	6.06	19.63	1.35	0.00	6.06	1 on 3
6-1	A	7/29/2014	9:52:54	NA	NA	14.52	12.84	Ind	Ind	0.00	ind	Ind
6-2	B	7/29/2014	9:30:54	NA	NA	14.52	12.62	3.39	0.23	12.62	8.12	1
6-3	D	7/30/2014	8:52:05	15	4	14.52	17.56	27.32	1.88	0.00	17.56	3
6-4	A	7/30/2014	10:07:36	15	4	14.52	16.55	Ind	Ind	0	16.55	Ind
6-5	A	7/30/2014	9:16:58	15	4	14.52	6.54	44.47	3.06	0.00	6.54	2
6-6	C	7/30/2014	9:25:54	15	4	14.52	8.29	37.26	2.57	0.00	8.29	1 on 3
7-1	B	7/29/2014	14:11:12	15	4	14.52	5.31	36.53	2.52	0.00	5.31	2 -> 3
7-2	B	7/29/2014	14:26:03	16	4	14.52	11.02	29.95	2.06	0.00	11.02	3
7-3	C	7/29/2014	14:41:14	16	4	14.52	8.21	34.48	2.38	0.00	8.21	2 on 3
7-4	A	7/30/2014	9:07:36	15	4	14.52	15.94	30.57	2.11	0.00	12.19	3
7-5	A	7/30/2014	9:12:37	15	4	14.52	4.68	35.39	2.44	0.00	4.68	2 on 3
7-6	B	7/30/2014	9:28:47	15	4	14.52	9.94	12.12	0.84	0.00	9.94	3
2-4_5	B	7/30/2014	14:20:17	15	4	14.52	15.13	13.55	0.93	0.00	6.06	1 -> 2
3-4_5	A	7/30/2014	12:14:18	15	4	14.52	11.44	40.84	2.81	0.00	11.44	3
4-4_5	B	7/30/2014	11:04:49	15	4	14.52	6.14	47.58	3.28	6.14	6.14	3
5-4_5	B	7/30/2014	9:57:48	15	4	14.52	6.06	25.57	1.76	6.06	6.06	2 -> 3
6_5-1	B	7/29/2014	10:11:37	NA	NA	14.52	12.71	Ind	Ind	0.00	ind	Ind
6_5-2	A	7/29/2014	10:03:55	NA	NA	14.52	4.10	0.00	0.00	4.10	ind	Ind
6_5-3	A	7/30/2014	8:12:53	16	4	14.52	5.47	Ind	ind	5.47	5.47	Ind
6_5-4	A	7/30/2014	8:25:48	16	4	14.52	15.29	18.36	1.27	IND	14.44	2 -> 3

Station	Replicate	Comment
1-1	B	silt sed; no GAC; thick layer of crab and mussel shells on surface; burrowing anemones; diver disturbance of SWI; transected burrows at depth
1-2	A	silt sed; no GAC; thick layer of crab and mussel shells on surface; diver disturbance of SWI; fecal pellets at SWI, relatively thick aRPD, transected burrows at depth
1-3	A	silty sed; no GAC; poor penetration due to shell armoring; transected burrows at depth
1-4	C	silt sed; no GAC; Draw down of tube worm tubes by camera prism, aRPD distorted by tube dragdown, evidence of Stage 3 at depth
1-5	C	Silt-clay; no GAC, small tubes @ SWI, evidence of transected burrows at depth, low density of deposit feeders present
1-6	A	Silt-clay, no GAC, transected burrows at depth
2-1	A	Silt-clay; no GAC; thick layer of shell fragments on surface; transected burrows at depth.
2-2	B	GAC pebbles and shell fragments on surface; hints of relict aRPD at lower left; profile disturbed by diver movement
2-3	A	Shell armoring over silt clay; former GAC location, so natural sedimentation has obliterated earlier GAC signal
2-4	B	Relict aRPD at depth, indicating GAC layer still in the process of being re-worked into the sediments; transected burrows at depth, no GAC pebbles visible
2-5	B	Silt clay with slight hint of remnant historic GAC layer at depth, but no obvious visible surface layer (completely reworked); transected burrows at depth.
2-6	A	Silt-clay with evidence of reworking at depth ; no hint of GAC presence; bioturbation exceeds prism penetration depth
3-1	A	Silt clay with thick surface armoring of shell hash; no GAC, cross-sectional detail disturbed by diver movement of prism; streaks on window from grease on diver glove
3-2	B	Silt-clay with shell armoring and GAC pebbles on surface; GAC layer exceeds prism penetration depth; cross-sectional detail disrupted by diver-movement of prism
3-3	C	Shell and cobble debris with disturbed profile from dragdown of surface armoring; impossible to measure aRPD, mixing depth, or successional stage in all 3 replicates collected at site.
3-4	A	Silt-clay with squid egg case on surface, transected burrows at depth with bioturbation exceeding prism penetration depth, no trace of GAC
3-5	C	Silty very fine sand with portions of polychaete visible against faceplate; bioturbation exceeds prism penetration depth.
3-6	C	Silty very fine sand over silt-clay; homogeneous subsurface texture, no trace of GAC, transected burrows at depth
4-1	B	Silt clay with thick surface armoring of shell hash; no GAC, cross-sectional detail disturbed by diver movement of prism; streaks on window from grease on diver glove
4-2	A	Silt clay with GAC particles at depth, GAC gravel near surface; large mussel and crab shell fragments on surface; small-medium shell fragments at depth; SWI disturbed by diver movement of prism.
4-3	A	Silt clay with thick surface layer of GAC particles and shells; reduced sediment at depth, both bioturbation & GAC layer exceed prism penetration depth
4-4	C	Silt clay with surface layer of GAC particles and shell fragments; reduced sediment at depth, both bioturbation & GAC layer exceed prism penetration depth
4-5	B	Silty fine sand over silt clay, no evidence of GAC, portions of polychaetes visible against faceplate, shallow burrowing bivalves in upper 3 cm
4-6	A	Silty fine sand over silt clay, no evidence of GAC, portions of polychaetes visible against faceplate, bioturbation exceeds prism penetration depth
5-1	B	Silt-clay; no GAC; thick layer of shell fragments on surface; transected burrows at depth; bioturbation exceeds prism penetration depth
5-2	A	Silt-clay with GAC gravel and some GAC particles visible; GAC exceeds prism penetration; dense mussel and crab shell on surface; a little diver disturbance of SWI

Station	Replicate	Comment
5-3	A	poor penetration, GAC greater than prism penetration depth
5-4	A	Sandy silt with GAC greater than prism penetration depth; both anemones and tube worms at surface
5-5	B	Silty fine sand with no GAC, transected burrows at depth, some shell fragments & anemones at SWI; bioturbation exceeds prism penetration depth
5-6	C	Silty fine to medium sand with no GAC; biorturbation exceeds prism penetration depth; shell fragments armoring surface
6-1	A	Sandy silt with thick layer of shell armoring on surface; detail in cross-sectional profile lost because of sampling artifact (diver prism motion)
6-2	B	Sandy silt with thick layer of GAC pebbles; GAC layer exceeds prism penetration depth; subsurface sediments extremely reduced; fine-scale structure obscured by prism movement by diver.
6-3	D	No GAC visible, but Beggiatoa on surface and evidence of transected burrows at depth, extending beyond prism penetration depth; high within-station variability among replicate images.
6-4	A	Sandy silt with surface disturbed/profile distorted from dragdown of anemones; Mussel shell in background, bioturbation appears to exceed prism penetration depth.
6-5	A	Silty fine sand, no GAC present; portions of polychaetes visible against faceplate at depth
6-6	C	Silty fine sand, no GAC present; portions of polychaetes visible against faceplate at depth, bioturbation exceeds prism penetration depth
7-1	B	Poorly sorted silty medium to coarse sand; no GAC, bioturbation exceeds prism penetration depth
7-2	B	Silty fine sand with no GAC, transected burrows at depth, shell/cobble armoring at SWI with some debris; bioturbation exceeds prism penetration depth
7-3	C	Silty fine sand with no GAC, transected burrows at depth, shell fragments at SWI; bioturbation exceeds prism penetration depth; portions of worms visible against faceplate at depth
7-4	A	Silty fine sand over silt clay; appears to be depositional layer (not GAC) of ca. 8-9 cm; some drag-down of sabellid tube on right edge of image
7-5	A	Silty fine to medium sand with no GAC; bioturbation exceeds prism penetration depth; some shell fragments on surface
7-6	B	Silty fine sand with no GAC; transected burrows at depth
2-4_5	B	Sandy silt with no apparent GAC, thin redox, looks like some activated carbon material at depth
3-4_5	A	Some shell fragments on surface, silty find sand, no GAC, subsurface organisms visible against faceplate at depth, bioturbation exceeds prism penetration depth
4-4_5	B	Bioturbation & GAC extends beyond penetration depth, GAC pebbles visible on surface, some remnants of activated carbon at depth; excellent recolonization recovery
5-4_5	B	Bioturbation & GAC extends beyond penetration depth, GAC pebbles visible on surface, reduced sediment from activated carbon at depth; excellent recolonization recovery
6_5-1	B	Silty sand & shell hash throughout entire profile, fine structure disturbed by diver artifact - no GAC present
6_5-2	A	All GAC with reduced sediment; too much disturbance to determine successional status or bioturbation mixing depth -- recolonization does look delayed compared with other stations.
6_5-3	A	All GAC but with well-oxygenated sediment (stark contrast to previous station); too many GAC pebbles to determine successional status
6_5-4	A	Sandy silt-clay with traces of activated carbon at depth; no distinct GAC layer with successful recolonization compared to previous survey